leading to the isolation of seven partial and one full-length *Unc5h1* cDNA and one full-length *Unc5h2* cDNA. Additional screens of E13 rat dorsal and ventral spinal cord libraries resulted in isolation of a second full-length *Unc5h2* cDNA as well as a nearly full-length *Unc5h1* cDNA. Sequencing was done on a Licor (L4000) automated sequencer as well as by ^{33}P cycle sequencing. Genbank accession numbers are U87305 and U87306 for rat *Unc5h1* and *Unc5h2*, respectively. RNA *in situ* hybridization was performed as described[13].

Antibodies, expression constructs and immunohistochemistry. Rabbit polyclonal antisera were raised against a peptide corresponding to a sequence (YLRKNFEQEPLAKE) in the extracellular domain of UNC5H1 that is almost completely conserved in UNC5H2 (one amino-acid substitution) and to peptides corresponding to unique sequences in the cytoplasmic domains of UNC5H1 (GEPSPDSWSLRLKKQ) and UNC5H2 (EARQQDDGDLNSLASA). Antisera were affinity-purified on their respective peptides (Quality Controlled Biochemicals). cDNAs for the various constructs were subcloned into the expression vectors pMT21 (Genetics Institute) and pCEP4 (Invitrogen) (for UNC5H1 and UNC5H2) or pRc/CMV (Invitrogen) (for RCM), and transiently transfected into 293 cells using lipofectamine. The antiserum to the extracellular peptide can detect UNC5H1 and UNC5H2 proteins expressed in transfected cells without cell permeabilization, whereas the antisera directed against the cytoplasmic domain peptides detected their respective proteins after cell permeabilization (data not shown). Netrin-1 protein was produced, purified, used and visualized in binding assays as described[13], except that a monoclonal antibody (9E10)[32] directed against a C-terminal Myc-epitope tag was used to detect recombinant netrin-1. Binding with netrin (VI·V)–Fc on 293T cells transiently transfected with UNC5H1, UNC5H2 or RCM was quantified essentially as described[13], except that after incubation with ligand, cells were washed once rapidly with 600 μl PBS and then fixed with 100% methanol followed by 4% paraformaldehyde. Cells were then washed once in PBS before proceeding with the secondary antibody incubation. The full-length UNC5H1 protein appears to be toxic for transfected 293 cells (data not shown), so binding experiments used a truncated UNC5H1 protein lacking a portion of the cytoplasmic domain (truncation at amino acid 494), which was not toxic. A 293-EBNA cell line stably expressing the UNC5H2–Fc fusion was derived and maintained as described[10,13]. The fusion protein was purified from serum-free medium conditioned for 7 d by affinity chromatography on protein A–agarose. The 293 cell line expressing netrin-1 has been described[10]. Binding of the UNC5H2–Fc fusion to this line was visualized using a Cy3-conjugated secondary antibody (Jackson Immunoresearch) directed against human Fc.

Received 4 December 1996; accepted 13 February 1997.

1. Ishii, N., Wadsworth, W. G., Stern, B. D., Culotti, J. G. & Hedgecock, E. M. UNC-6, a laminin related protein, guides cells and pioneer axon migrations in *C. elegans*. *Neuron* **9**, 873–881 (1992).
2. Serafini, T. *et al.* The netrins define a family of axon outgrowth-promoting proteins homologous to *C. elegans* UNC-6. *Cell* **78**, 409–424 (1994).
3. Kennedy, T. E., Serafini, T., de la Torre, J. R. & Tessier-Lavigne, M. Netrins are diffusible chemotropic factors for commissural axons in the embryonic spinal cord. *Cell* **78**, 425–435 (1994).
4. Colamarino, S. A. & Tessier-Lavigne, M. The axonal chemoattractant netrin-1 is also a chemorepellent for trochlear motor axons. *Cell* **81**, 621–629 (1995).
5. Shirasaki, R., Tamada, A., Katsumata, R. & Murakami, F. Guidance of cerebellofugal axons in the rat embryo: directed growth toward the floor plate and subsequent elongation along the longitudinal axis. *Neuron* **14**, 961–972 (1995).
6. Wadsworth, W. G., Bhatt, H. & Hedgecock, E. M. Neuroglia and pioneer neurons express UNC-6 to provide global and local netrin cues for guiding migrations in *C. elegans*. *Neuron* **16**, 35–46 (1996).
7. Mitchell, K. J. *et al.* Genetic analysis of *Netrin* genes in *Drosophila*: Netrins guide CNS commissural axons and peripheral motor axons. *Neuron* **17**, 203–215 (1996).
8. Harris, R., Sabatelli, L. M. & Seeger, M. A. Guidance cues at the *Drosophila* CNS midline: identification and characterization of two *Drosophila* Netrin/UNC-6 homologs. *Neuron* **17**, 217–228 (1996).
9. Serafini, T. *et al.* Netrin-1 is required for commissural axon guidance in the developing vertebrate nervous system. *Cell* **87**, 1001–1014 (1996).
10. Shirasaki, R., Mirzayan, C., Tessier-Lavigne, M. & Murakami, F. Guidance of circumferentially growing axons by netrin-dependent and -independent floor plate chemotropism in the vertebrate brain. *Neuron* **17**, 1079–1088 (1996).
11. Chan, S. S.-Y. *et al.* UNC-40, a *C. elegans* homolog of DCC (Deleted in Colorectal Cancer), is required in motile cells responding to UNC-6 netrin cues. *Cell* **87**, 187–195 (1996).
12. Kolodziej, P. A. *et al. frazzled* encodes a *Drosophila* member of the DCC immunoglobulin subfamily and is required for CNS and motor axon guidance. *Cell* **87**, 197–204 (1996).
13. Keino-Masu, K. *et al. Deleted in Colorectal Cancer* (*DCC*) encodes a netrin receptor. *Cell* **87**, 175–185 (1996).
14. Leung-Hagesteijn, C. *et al.* UNC-5, a transmembrane protein with immunoglobulin and thrombospondin type 1 domains, guides cell and pioneer axon migrations in *C. elegans*. *Cell* **71**, 289–299 (1992).
15. Fazeli, A. *et al.* Phenotype of mice lacking functional Deleted in Colorectal Cancer (*DCC*) gene. *Nature* **386**, 796–804 (1997).
16. Hedgecock, E. M., Culotti, J. G. & Hall, D. H. The *unc-5*, *unc-6* and *unc-40* genes guide circumferential migrations of pioneer axons and mesodermal cells on the epidermis in *C. elegans*. *Neuron* **2**, 61–85 (1990).
17. McIntire, S. L., Garriga, G., White, J., Jacobson, D. & Horvitz, H. R. Genes necessary for directed axonal elongation or fasciculation in *C. elegans*. *Neuron* **8**, 307–322 (1992).
18. Hamelin, M., Zhou, Y., Su, M. W., Scott, I. M. & Culotti, J. G. Expression of the UNC-5 guidance receptor in the touch neurons of *C. elegans* steers their axons dorsally. *Nature* **364**, 327–330 (1993).
19. Ackerman, S. L. *et al.* The mouse rostral cerebellar malformation gene encodes an UNC-5 like protein. *Nature* **386**, 838–842 (1997).
20. Willott, E. *et al.* The tight junction protein ZO-1 is homologous to the *Drosophila* discs-large tumor suppressor protein of septate junctions. *Proc. Natl Acad. Sci. USA* **90**, 7834–7838 (1993).
21. Itoh, M. *et al.* The 220-kD protein colocalizing with cadherins in non-epithelial cells is identical to ZO-1, a tight junction-associated protein in epithelial cells: cDNA cloning and immunoelectron microscopy. *J. Cell Biol.* **121**, 491–502 (1993).
22. Sheng, M. PDZs and receptor/channel clustering: rounding up the latest suspects. *Neuron* **17**, 575–578 (1996).
23. Altman, J. & Bayer, S. A. The development of the rat spinal cord. *Adv. Anat. Embryol. Cell Biol.* **85**, 1–166 (1984).
24. Ramón y Cajal, S. *Histologie du Système Nerveux de l'Homme at des Vertébrés* Vol. 2 (Maloine, Paris, 1911).
25. Rakic, P. Neuron–glia relationship during granule cell migration in developing cerebellar cortex. A Golgi and electron microscopic study in *Macacus rhesus*. *J. Comp. Neurol.* **141**, 283–312 (1971).
26. Klar, A., Baldassare, M. & Jessell, T. M. F-spondin: a gene expressed at high levels in the floor plate encodes a secreted protein that promotes neural cell adhesion and neurite extension. *Cell* **69**, 95–110 (1992).
27. Messersmith, E. K. *et al.* Semaphorin III can function as a selective chemorepellent to pattern sensory projections in the spinal cord. *Neuron* **14**, 949–959 (1995).
28. Luo, Y., Raible, D. & Raper, J. A. Collapsin: a protein in brain that induces the collapse and paralysis of neuronal growth cones. *Cell* **75**, 217–227 (1993).
29. Guthrie, S. & Pini, A. Chemorepulsion of developing motor axons by the floor plate. *Neuron* **14**, 1117–1130 (1995).
30. Varela-Echavarria, A., Tucker, A., Puschel, A.& Guthrie, S. Motor axon subpopulations respond differentially to the chemorepellents netrin-1 and semaphorin D. *Neuron* **18**, 193–207 (1997).
31. Livesey, F. J. & Hunt, S. P. Netrin and netrin receptor expression in the embryonic mammalian nervous system suggests role in retinal, striatal, nigral and cerebellar development. *Mol. Cell. Neurosci.* (in the press). **UPDATE?**
32. Evan, G. I., Lewis, G. K., Ramsay, G. & Bishop, J. M. Isolation of monoclonal antibodies specific for human *c-myc* proto-oncogene product. *Mol. Cell. Biol.* **5**, 3610–3616 (1985).

Acknowledgements. We thank A. Faynboym for purification of netrin proteins, C. Mirzayan for the 293 cell line expressing netrin-1, D. Shehu for sequencing, V. Head for assistance with *in situ* hybridization, and S. Nakanishi for the brain cDNA library. Supported by grants to M.T.-L. from the International Spinal Research Trust, the American Paralysis Association and the Howard Hughes Medical Institute, and to S.L.A. from the NIH. E.D.L. was supported by a UCSF chancellor's fellowship, L.H. by a fellowship from the Jane Coffin Childs Memorial Fund, and K.K.-M. by the National Defense Medical College, Japan. M.M. is an associate and M.T.-L. an Investigator of the Howard Hughes Medical Institute.

Correspondence and requests for materials should be addressed to M.T.-L. (e-mail: marctl@itsa.ucsf.edu).

The mouse rostral cerebellar malformation gene encodes an UNC-5-like protein

Susan L. Ackerman, Leslie P. Kozak, Stefan A. Przyborski, Laurie A. Rund*, Bert B. Boyer* & Barbara B. Knowles

The Jackson Laboratory, Bar Harbor, Maine 04609, USA

Migration of neurons from proliferative zones to their functional sites is fundamental to the normal development of the central nervous system[1,2]. Mice homozygous for the spontaneous rostral cerebellar malformation mutation (*rcm*^{s}) or a newly identified transgenic insertion allele (*rcm*^{tg}) exhibit cerebellar and midbrain defects, apparently as a result of abnormal neuronal migration. Laminar structure abnormalities in lateral regions of the rostral cerebellar cortex have been described in homozygous *rcm*^{s} mice[3]. We now demonstrate that the cerebellum of both *rcm*^{s} and *rcm*^{tg} homozygotes is smaller and has fewer folia than in the wild-type, ectopic cerebellar cells are present in midbrain regions by three days after birth, and there are abnormalities in postnatal cerebellar neuronal migration. We have cloned the *rcm* complementary DNA, which encodes a transmembrane receptor of the immunoglobulin superfamily. The sequence of the *rcm* protein (Rcm) is highly similar to that of UNC-5, a *Caenorhabditis elegans* protein that is essential for dorsal guidance of pioneer axons and for the movement of cells away from the netrin ligand, which is encoded by the *unc-6* gene[4–7]. As Rcm is a member of a newly

* Present addresses: Department of Biochemistry, University of Illinois, Urbana, Illinois 61801, USA (L.A.R.); The Institute of Arctic Biology, University of Alaska, Fairbanks, Alaska 99775, USA (B.B.B.).

described family of vertebrate homologues of UNC-5 which are netrin-binding proteins, our results indicate that UNC-5-like proteins may have a conserved function in mediating netrin-guided migration[8].

Ataxia was observed in some of the offspring from heterozygous matings of one (line 1.23) of three lines of mice transgenic for a mitochondrial uncoupling protein (*Ucp*) minigene. Histological analysis of these homozygous transgenic mice revealed cerebellar abnormalities. Complementation tests in which mice heterozygous for the transgenic lineage 1.23 were mated to heterozygous rcm^{s} mice, produced several offspring exhibiting the abnormal gait characteristic of both homozygous 1.23 transgenic mice and homozygous rcm^{s} mice. On the basis of these results, we assumed that the *Ucp* minigene disrupted the *rcm* locus in this lineage.

A dramatic reduction in cerebellar size and in the number of folia was observed in midline sagittal sections of cerebella from homozygous rcm^{tg} and rcm^{s} adults (Fig. 1). This size reduction was more pronounced in rcm^{tg} than in rcm^{s} homozygotes. Vermal fissure development in rcm^{tg} and rcm^{s} homozygotes resulted in the formation of only five or six lobes, respectively, compared with the eight major lobes seen in the control wild-type mice, $rcm^{tg}/+$ and $+/+$ (B6C3). Fissure formation was also abnormal in the lateral cerebellar hemispheres of both rcm^{s}/rcm^{s} and rcm^{tg}/rcm^{tg} mice, a disruption that was more severe in the rcm^{tg} homozygote (Fig. 1). The effects of both the rcm^{tg} and rcm^{s} mutations on fissure development were evident at birth (P0) and fissure development continued to be delayed during the postnatal period. The cerebella of mutant mice were smaller at birth, suggesting that the *rcm* gene may play a role in cell proliferation during embryogenesis (data not shown).

The most striking defect in the brain of *rcm* homozygotes was found in lateral regions where the inferior colliculus adjoins the cerebellum. An abnormal band of granule cells extending from the cerebellum and continuing into the inferior colliculus was observed in sagittal sections lateral to midline. Analysis of the more lateral sections revealed partial fusion of the inferior colliculus and the rostral cerebellum and a number of ectopic granule and calbindin-positive Purkinje cells in the inferior colliculus and tegmentum of the midbrain (Fig. 1, and data not shown). These ectopic cells were not found in the adjoining superior colliculus or thalamus, suggesting that incursion of cerebellar cells into these regions is blocked during brain development. To determine when during development these ectopic granule and Purkinje cells arise, we did an *in situ* analysis of serial sections from rcm^{s}/rcm^{s} embryos at embryonic days 13.5, 15.5 and 17.5 and at postnatal days P0, P3 and P7, using a antisense probe for *Math1*, a basic helix–loop–helix protein expressed in external granular cells[9,10]. Ectopic granule cells were first detected at P3, the time when these cells normally begin their postnatal migration, and had increased in number by P7 (Fig. 2a). Ectopic Purkinje cells were not detected at P0 but were found at P3 (Fig. 2b). Both ectopic granule and Purkinje cells expressed the *rcm* transcript (data not shown), supporting a cell-autonomous role for the *rcm* protein.

Defects in the laminar structure of rcm^{tg}/rcm^{tg} and rcm^{s}/rcm^{s} cerebella were observed by P7. Abnormal external granule cell migration, characterized by the appearance of cohorts rather than individual cells migrating across the molecular layer, was clearly evident in some lateral areas of the cerebellum (Fig. 2c). These aggregates of cells that extend into the inner granule layer were often associated with gaps in the Purkinje cell layer. The movement of ectopic Purkinje and granule cells into the midbrain by P3, together with the presence of aberrant cohorts of granule cells postnatally and the abnormal laminar structure in the adult cerebellum, suggest a role for the *rcm* gene in neuronal migration.

To isolate the *rcm* gene, a genomic DNA fragment flanking the transgene insertion site was identified (Fig. 3a). Restriction-fragment length polymorphisms were detected by analysis of DNA from rcm^{tg} homozygotes and wild-type mice using the flanking fragment as a probe. Analysis of DNA from an interspecific backcross mapping panel confirmed that this fragment was derived from the region of chromosome 3 known to contain the *rcm* gene[11]. Two P1 clones containing this flanking sequence were identified and genomic fragments that overlapped with the 8-kilobase (kb) *Xba*I fragment were isolated and used as probes on Southern blots containing wild-type and rcm^{tg}/rcm^{tg} genomic DNA. Both this analysis and polymerase chain reaction (PCR) studies using primers corresponding to these fragments indicated that ~8.5 kb of DNA adjacent to the transgene insertion site was deleted (Fig. 3a, dashed line).

Northern blots of adult brain RNA were probed with genomic DNA fragments corresponding to sequences within the deletion in

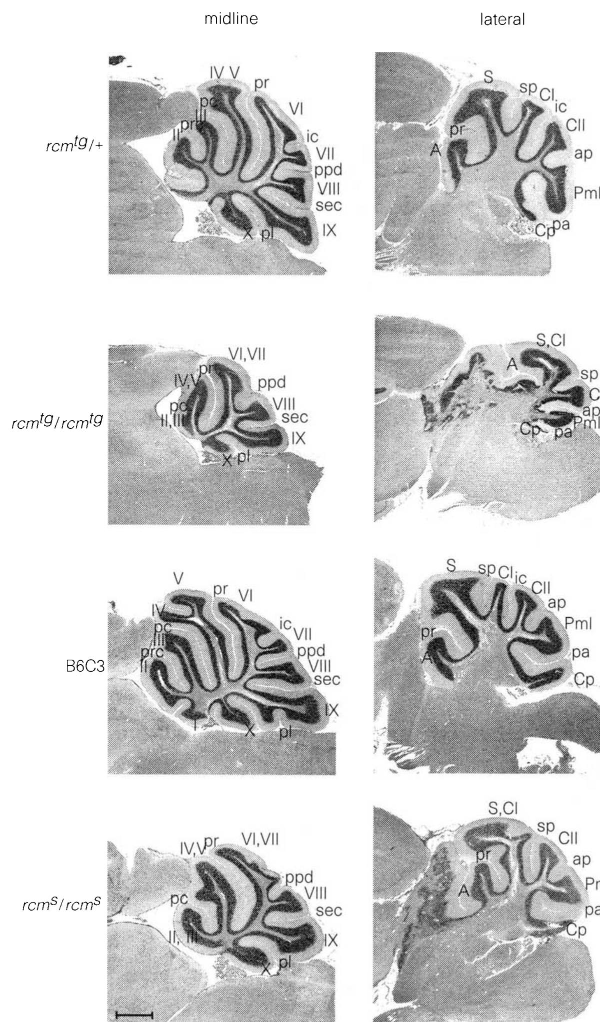

Figure 1 Defects in the *rcm* gene result in abnormalities in foliation and laminar structure of the adult cerebellum. Haematoxylin- and -eosin-stained sagittal sections from midline and lateral regions of wild-type ($rcm^{tg}/+$ and B6C3 Fe *a/a* (B6C3)) or mutant (rcm^{tg}/rcm^{tg} and rcm^{s}/rcm^{s}) cerebella are shown. The lateral ventricles and hippocampus were used as landmarks for the lateral sections. Anterior is to the left and dorsal to the top in each photograph. Roman numerals I–X indicate vermal lobes. Fissures are abbreviated as follows: prc, precentral; pc, preculminary; pr, primary; ic, intercrural; ppd, prepyramidal; sec, secondary; pl, posterolateral; sp, superior posterior; ap, ansoparamedial; and pa, paraflocculilaris. Hemispheric lobes are as follows: A, anterior; S, simplex; CI, crus I; CII, crus II; Pml, paramedial. In midline sections, note the absence of the precentral fissure in the anterior region and the intercrural fissure in the medial posterior region (in midline and lateral sections) in both rcm^{tg} and rcm^{s} homozygotes and the poor development of the preculminate fissure in rcm^{tg} homozygotes. Scale, 670 μm.

order to identify candidate exons. Both the 1.7-kb *Xba*I fragment (Fig. 3a, hatched box) and an adjacent 5.5-kb *Xba*I fragment (not shown) detected a transcript of ~9.3 kb in wild-type adult brain. DNA sequence analysis of the 1.7-kb *Xba*I fragment using the GRAIL 1A gene analysis program indicated the presence of a 110-base-pair (bp) putative exon. cDNA clones encompassing 9.3 kb of sequence were isolated by 5′ and 3′ RACE (rapid amplification of cloned ends) using adult brain cDNA. A corresponding transcript was not detected by northern blot analysis of adult cerebellar messenger RNA isolated from homozygous rcm^{tg} animals, whereas a similar amount of transcript was detected in rcm^{s}/rcm^{s} and wild-type adults (Fig. 3b).

To test the rcm^{s} transcript for mutations, PCR analysis with reverse transcription (RT-PCR) was done on rcm^{s}/rcm^{s} and wild-type cerebellar cDNA with primers designed from the putative open reading frame. Primers corresponding to a region of the candidate gene encoding the C terminus of the protein amplified a band from rcm^{s} that was ~160 bp larger than that from wild-type cDNA (data not shown). Sequence analysis revealed a tandem duplication of an exon encoding amino acids 763–818 that did not disrupt the

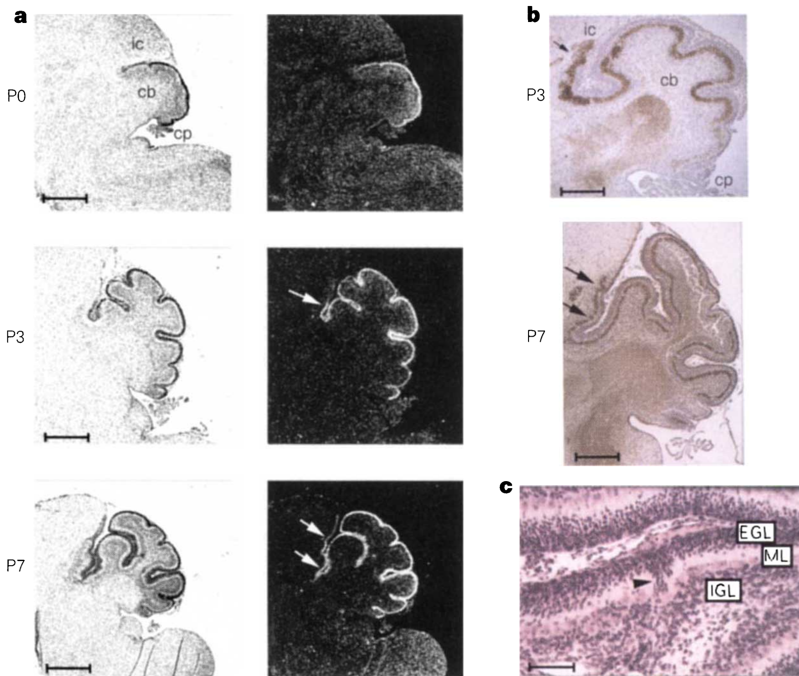

Figure 2 Midbrain and neuronal migration defects in rcm^{tg}/rcm^{tg} mice. Anterior is to the left and dorsal to the top. **a**, *In situ* analysis of parasagittal sections through the inferior colliculus (ic) and cerebellum (cb) using *Math1* as probe. Corresponding bright-field and dark-field images are shown. Arrows denote granule cells in midbrain regions of rcm^{s}/rcm^{s} animals. Such cells were not detected in wild-type controls. Scale bars, 5.5 mm in P0 and P3, and 8.0 mm in P7. **b**, Immunohistochemical analysis of Purkinje cells in parasagittal sections of postnatal rcm^{s}/rcm^{s} brains after reaction with calbindin antiserum. Sections were counterstained with haematoxylin to show granule cells. Scale bars, 3.0 mm (P3) and 4.8 mm (P7). **c**, Parasagittal section through a P7 cerebellum. Note the presence of an abnormal cohort of granule cells (large arrowheads) and normal, individual granule cells (small arrowheads) in the molecular layer, EGL, external granule layer; ML, molecular layer; IGL, internal granule layer. Scale bar, 1.6 mm.

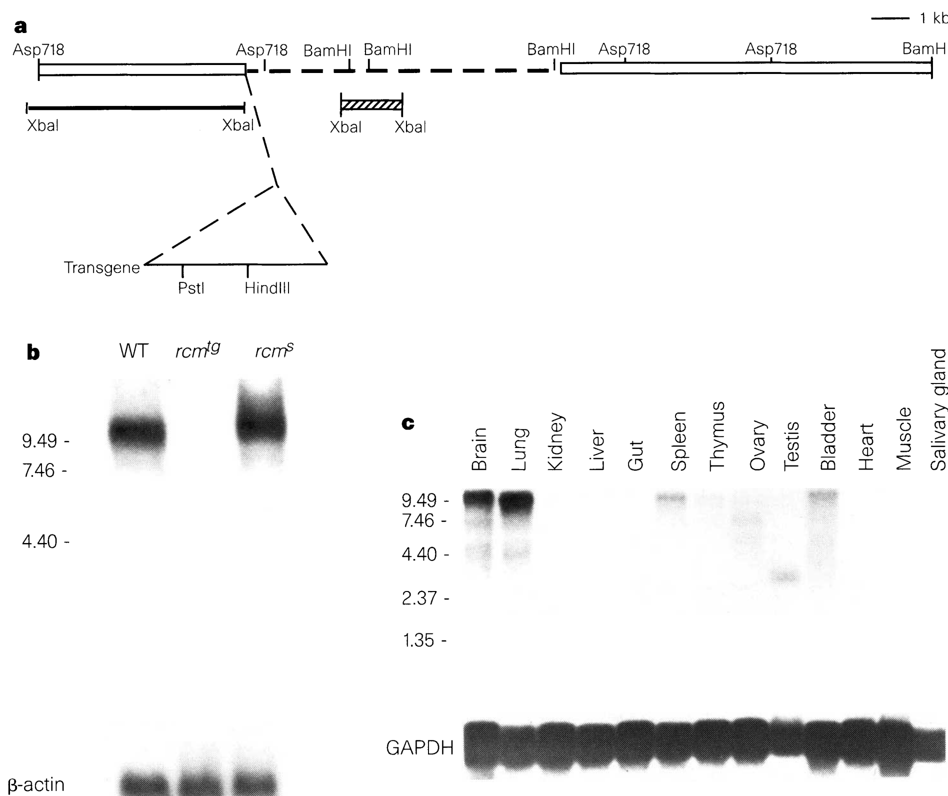

Figure 3 Molecular characterization of the rcm^{tg} mutation and the expression pattern of the *rcm* transcript in adult tissues and developing cerebellum. **a**, Map of the genomic DNA surrounding the *Ucp1* transgene insertion. White bars represent genomic DNA, dashed line indicates the 8.5-kb deletion adjacent to the transgene insertion. Solid line represents the original 8-kb *Xba*I fragment isolated from the rcm^{tg} genomic library; the hatched box indicates the 1.7-kb *Xba*I fragment containing the exon identified by GRAIL. **b**, Northern blot analysis of 10 μg poly(A)$^{+}$ RNA from the cerebella of wild-type (WT), rcm^{tg}/rcm^{tg}, and rcm^{s}/rcm^{s} mice. The blot was probed with a 0.7-kb *rcm* partial cDNA fragment and reprobed with β-actin as a control. **c**, Northern blot of poly(A)$^{+}$ RNA (10 μg) extracted from normal adult mouse tissues hybridized to a ^{32}P-labelled 582-bp *rcm* cDNA fragment. The blot was exposed to X-ray film at −70 °C for 2.5 days. Lower panel, same blot rehybridized to a GAPDH probe and exposed for 5 h. RNA size markers (Gibco BRL) are shown on the left.

a

```
       Ig-like   Ig-like  TSP-1 TSP-1 TM
[Sig]--[     ]---[     ]--[    |    ][■]------------------------------
```

b

```
RCM    MRKGLRATAARCGLGLGYLLQMLVLPALALLSASGTGSAAQDDEFFHELPETFPSDPPEPLPHFLIEPEEAYIVK  75
UNC-5  M-------------------------------------------DEI------TTT-----------QPKSGYVIR  17

RCM    NKPVNLYCKASPATQIYFKCNSEWVHQKDHVVDERVDETSGLIVREVSIEISRQQVEELFGPEDYWCQCVAWSSA  149
UNC-5  NKPLRLQCRANHATKIRYKCSSKWIDDSRIEKLIGTDSTSGVGYIDASVDISRIDVDSTGHVDAFQCQCYASGDD  92

RCM    GTTK--SRKAYVRIAYLRKTFEQEPLGKEVSLEQEVLLQCRPPEGIPVAEVEWLKNEDIIDPAEDRNPYITIDHN  222
UNC-5  DQDVVASDVATVHLAYMRKHELKSPVAQRVQEGTTLQLPCQAPESDPKAELTWYKDGVVVQP--DANVIRASDGS  165

RCM    LIIKQARLSDTANYTCVAKNIVAKRKSTTATVIVYVNGGWSTWTEWSV----------------CNSRCGRGYQK  281
UNC-5  LIMSAARLSDSGNYTCEATNVANSRKTDPVEVQIYVDGGWSEWSPWIGTCHVDCPLLRQHAHRIRDPHDVLPHQR  240

RCM    RTRTCTNPAPLNGGAFCEGQSVQKIACTTLCPVDGRWTSWSKWSTCGTECTHWRRRECTAHAPKNGGKDCDGIVL  356
UNC-5  RTRTCNNPAPLNDGEYCKGEEEMTRSCKVPCKLDGGWSSWSDWSACSSSCHRYRTRACTVPEPNNGGQPCEGDDL  315

RCM    QSKNCTDGLCMQAAPDSD--DVALYVGIVIAVTVCLAITVVVALF---VYRKNHRDFESDIIDSSALNGGFQPV  425
UNC-5  MTQECPAQLCTADSSRIVISDTAVYGSVASIFIVASFLLAILAMFCCKRGNSKKSKPLKPQKMNS-EDAGGTYYS  389

RCM    NIKAARQDLLAVPPDLTSAAAMYRGPVYALHDVSDKIPMTNSPILDPLPNLKIKVYNSSGAVTPQDDLAEFSS--  498
UNC-5  EPPGVRRLLLEHQHGTLLGEKISSCSQYFEPPPLPHSTTLRSGKSAFSGYSSTRNAGSRAALIQECSSSSSGSGG  464

RCM    KLSPQMTQSLLENEALN-------LKNQSLARQTDPSCTAFGTFNSLGGHLIIPNSGVSLLIPAGAIPQGRVYEM  567
UNC-5  KRTMLRTSSSNCSDDDNYATLYDYMEDKSVLGLDTSQNIVAAQIDSNGARLSLSKSGARLIVPELAVEGEKMLYL  539

RCM    YVTVHRKENMRP-PMEDSQTLLTPVVSCG----PPGALLTRPVILTLHHCADPSTED-WKIQLKNQAVQGQWEDV  636
UNC-5  AVSDTLTDQPHLKPIESALSPVIVIGQCDVSMSAHDNILRRPVVVSFRHCASTFPRDNWQFTLYADEGSG-WQKA  613

RCM    VVVGEENFTTPCYIQLDAEA--------CHILTENLSTYALVGQSTTKA--AAKRLKLAIFGP--LCCSSLEYSI  699
UNC-5  VTIGEENLNTNMFVQFEQPGKKNDGFGWCHVMTYSLARLMLAGHPRRNSLSAAKRVHLAVFGPTEMSAYRRPFEL  688

RCM    RVYCLDDTQDALKEVLQLERQMGGQLLEEPKALHFKGSIHNLRLSIHDIAHSLWKSRLLAKYQEIPFYHIWSGSQ  774
UNC-5  RVYCVPETGAAMESVWKQED--GSRLLCESNDFILNE-KGNLCICLEDVIPGF--SCDGPEVVRISETQHRFVAQ  758

RCM    RNLHCTFTLERLSLNTVELVCKLCVRQVEGEGQIFQLNCTVSEEPTGIDLPLLDPASTITTVTGRSAFSIPLPIR  849
UNC-5  NGLHCSLKFRPKEIN----GSQFSTRVIVYQ----KASSTEPMVMEVSNEPELYDATSEEREKGSVCVEFRLPEG  825

RCM    QK--LCSSLDAPQTRGHDWRMLAHKLNLDRYLNYFAT--KSSPTGVILDLWEAQNF-PDGNLSMLAAVLEEMGRH  919
UNC-5  VKDELARLLDMPNESHSDWRGLAKKLHYDRYLQFFASFPDCSPTSLLLDLWEASSSGSARAVPDLLQTLRVMGRH  900

RCM    ETVV----SLAAEGQY--- 931
UNC-5  DAVMVLERFLSAFPQIVSP 919
```

c

```
ZO-1  TARGIFNSNGGYLSSIETGVSIIIPQGAIPEGIEQEIYFKVQRDNSILPPLDKEKGETLLSPLVMCGPHGLKFLKPVELRLPHC  1715
RCM   TAFGTFNSLGGHLIIPNSGVSLLIPAGAIPQGRVYEMYVTVHRKENMRPPME--DSQTLLTPVVSCGPPGALLTRPVILTLHHC  617
```

Figure 4 RCM protein structure. **a**, Domain structure of the RCM protein. An N-protein signal sequence (Sig) with a consensus cleavage site at residue 40 was detected by hydrophobicity and signal analysis[21,22]. A hydrophobic region of 24 amino acids (residues 377–400), predicted to be the single membrane-spanning region based on ALOM analysis, is flanked by charged residues on both the N- and the C-terminal sides, indicating that the RCM protein adopts a type Ia ($N_{exo}C_{cyto}$) orientation[23,24]. TSP-1, thrombospondin type-1; TM, transmembrane domain. **b**, RCM and UNC-5 amino-acid sequence homology. Identical (boxed and shaded) and similar (shaded only) amino acids between the mouse RCM and *C. elegans* UNC-5 proteins. Alignment was performed using the ALIGN program (FASTA). The lack of homology in the most N-terminal region of the RCM protein probably reflects the putative signal sequence in the RCM protein that is not found in UNC-5. **c**, RCM and ZO-1 amino-acid sequence homology. Identical (shaded and boxed) and similar (shaded only) amino acids in the C-terminal region of the mouse RCM and the mouse ZO-1 proteins. The region is also conserved in the human ZO-1 protein.

reading frame but resulted in a putative Rcm protein containing an additional 55 amino acids. Southern blot analysis of wild-type and homozygous rcm^s DNA using this exon as a probe confirmed the presence of this duplication in the genome of rcm^s/rcm^s mice (data not shown).

Northern blot analysis of the *rcm* transcript in adult mouse tissues indicated that expression was highest in brain and lung (Fig. 3c). Less *rcm* RNA was detected in testis, ovary, thymus, spleen and bladder; upon longer exposure (>7 days), transcripts were also detected in kidney, intestine and salivary gland. In addition to the predominant 9.3-kb band seen in most tissues, two additional transcripts of 6.0 kb and 4.4 kb were present from ovary; testis expresses a single band of 3.4 kb.

Sequence analysis of *rcm* cDNA clones detected an open reading frame encoding a 931-amino-acid transmembrane protein with a predicted relative molecular mass of 103K. BLASTP analysis detected two immunoglobulin (Ig)-like domains (residues 76–151 and 181–246) and two thrombospondin (TSP) type-1 motifs (residues 259–315 and 316–369) within the 377-amino-acid extracellular region (Fig. 4a). This unique combination of immunoglobulin and TSP-1 domains in the extracellular region is very similar to the *C. elegans* UNC-5 transmembrane protein involved in cell migration[5]. Amino-acid sequence comparison of the Rcm and UNC-5 transmembrane protein also revealed a high homology (29.5% identity and 72.8% similarity between residues 66–931) (Fig. 4b). This sequence and structure homology between Rcm and UNC-5 strongly supports our idea that Rcm is involved in cerebellar neuronal migration. Although the intracellular region of Rcm appears to have no discernible domain structure, the amino-acid sequence between residues 531–612 is 48% identical (65% similarity) to the mouse and human tight-junction protein ZO-1 (Fig. 4c). ZO-1 contains both SH3 and guanylate kinase-like domains, and may be involved in signal transduction at specialized cell–cell junctions[12].

The *rcm* transcript is temporally and spatially regulated during postnatal granule cell migration. *In situ* hybridization analysis of P0 brain detected high levels of *rcm* mRNA in the cerebellum (Fig. 5a). Cerebellar *rcm* expression appeared to peak at P7 (Fig. 5d) and was significantly downregulated by P21 (Fig. 5f), by which time granule-cell migration is complete. In the P0 cerebellum, *rcm* expression was detected in granule-cell precursors in the external granule layer as well as in Purkinje cells. At P7, *rcm* expression was detectable in cells of both the superficial proliferating zone of the external granule layer and in those of the premigratory zone. Expression was also seen in migrating granule cells within the molecular layer, post-migratory cells in the internal granule layer, and in Purkinje cells. The *rcm* transcript is therefore expressed in the cells that undergo aberrant migration during the period in which these migrations occur. Although the level of *rcm* expression in granule neurons significantly decreased by P21, it was maintained in Purkinje cells and remained detectable in these neurons in the adult brain. Cerebellar expression appeared uniform with respect to rostral/caudal and medial/lateral axes. *rcm* transcripts were also detected in the olfactory bulb and the dentate gyrus of the hippocampus, whereas the pontine and olivary nuclei expressed lower levels of the transcript (Fig. 5a). Obvious abnormalities in these structures were not detected in *rcm* homozygotes.

Genetic studies in *C. elegans* indicate that the UNC-5 receptor interacts with the netrin ligand encoded by *unc-6* (refs 4, 6). Netrins promote outgrowth of rat spinal cord commissural axons *in vitro*[13]. *In vivo*, netrin-1 is not only required for guidance of spinal commissural axons, but also for the formation of the pontine nuclei and several brain commissures, indicating a role for this molecule in both cell migration and axonal guidance in the developing brain[14]. The Rcm protein binds netrin-1 *in vitro*[8]. The fact that netrin-1 is expressed during embryonic and postnatal development of the rat cerebellum also supports a role for it as an Rcm ligand *in vivo*[15].

Our results indicate that Rcm protein and its ligand are important in critical migratory and/or cell proliferation events during cerebellar development. The *rcm* mutations only affect the migration of a subset of *rcm*-expressing cells in the developing brain, an

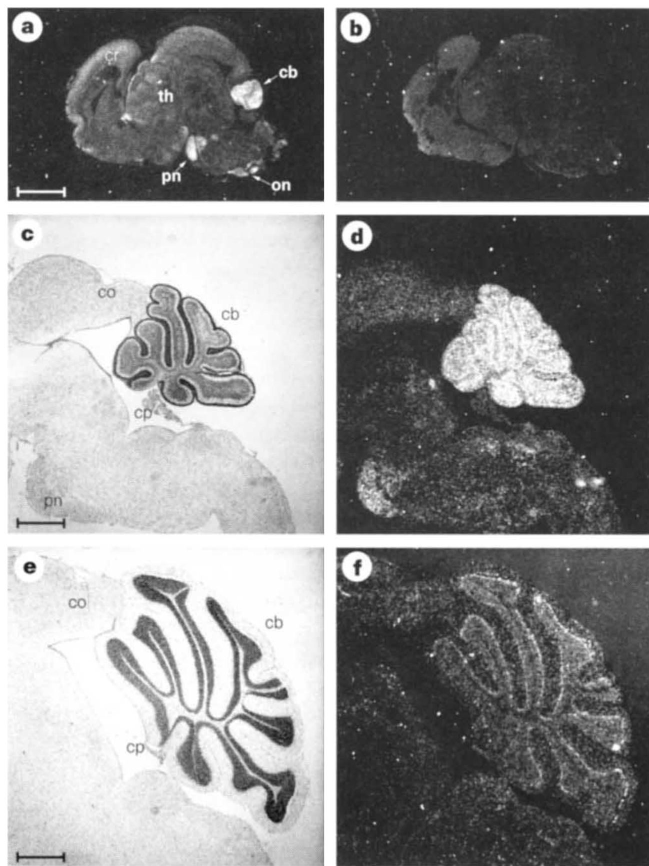

Figure 5 Localization of *rcm* transcript by *in situ* hybridization of mid-sagittal sections of normal neonatal mouse brain. Dark-field images of adjacent sections of P0 brain demonstrate the localization of the signal after hybridization with antisense (**a**) and the negative control sense (**b**) strand *rcm* probes. Bright-field (**c**, **e**) and corresponding dark-field (**d**, **f**) micrographs illustrate the expression pattern of the antisense *rcm* probe in P7 (**c**, **d**) and P21 (**e**, **f**) cerebellum. Abbreviations: cb, cerebellum; cp, choroid plexus; co, colliculi; cr, cerebral hemisphere; pn, pontine nuclei; on, olivary nuclei; th, thalamus. Scale bars represent 1.25 mm (**a**, **b**) and 0.65 mm (**c–f**).

observation that implies genetic redundancy as the expression domains of *rcm* within the cerebellum and other regions of the developing brain overlap with those of *Unc5 h-1* and *Unc5 h-2*, two other members of the vertebrate UNC-5-like gene family[8]. □

Methods

Mice. rcm^{tg}/rcm^{tg} animals were derived from a previously described *Ucp1* transgenic mouse lineage produced and maintained on a C57BL/6J × SJL/J background[16]. rcm^{s}/rcm^{s} mice were obtained from the Mouse Mutant Resource at The Jackson Laboratory. This mutation arose on a C57BL/6J background and is currently maintained on an F_1 hybrid B6C3HFe-*a/a* background.

Histology and immunohistochemistry. For histological examination, 7–10 adult mice were perfused with Bouin's solution, cerebella were removed and then postfixed overnight. Neonatal brains (3–4 at each time point) were immersion-fixed in paraformaldehyde. Slides were examined on a Leica DMRXE microscope and high-resolution digital images were recorded by a Kodak Megaplus 1.4 camera.

Sections were incubated overnight at 4 °C with rabbit polyclonal antiserum against calbindin-D (Swant), diluted 1 : 1,500. Antibody binding was detected using biotinylated anti-rabbit IgG biotin conjugate (Sigma) diluted 1 : 50, and the ExtrAvidin peroxidase staining kit using DAB as enzyme substrate (Sigma).

Genomic library construction and genetic mapping. The genomic DNA library was prepared by ligation and packaging of *Mbo*I partially digested spleen DNA from a homozygous rcm^{tg} mouse, according to the manufacturer's protocol. Positive clones were identified by hybridization to a 1.8-kb *Pst*I/*Hind*III fragment of the *Ucp1* transgene[16]. P1 clones were isolated from a 129 ES cell library[17].

5′ and 3′ RACE analysis. PCR reactions were done with Marathon RACE-ready cDNA and KlenTaq Polymerase (Clontech) according to the manufacturer's protocol. Products were ligated into the TA-cloning vector PCR II (Invitrogen), and sequenced on the ABI 373 Stretch DNA sequencer using dideoxyterminator chemistry.

Northern blot analysis. Total RNA was prepared from tissues by the guanidinium isothiocyanate method and poly(A)$^+$ RNA was isolated using oligo(dT) cellulose[18]. RNA was electrophoresed through formaldehyde gels and transferred to nylon filters (Magna, MSI) by standard methods. Membranes were hybridized and washed as described[19].

***In situ* hybridization.** ^{33}P-labelled sense and antisense riboprobes (10^5 c.p.m. μl^{-1}) were generated from a plasmid containing 582 bp of the coding region of the RCM cytoplasmic domain or 1.1 kb of the *Math1* open reading frame. Sample preparation, hybridization, and post-hybridization washes were as described except that hybridizations were done at 50 °C and the initial wash in 50% formamide/2 × SSC was for 2 h at 37 °C[20]. Slides were dipped in Kodak NTB 2 emulsion, exposed for 24 h at 4 °C, and developed in Kodak D19. Sections were stained with haematoxylin and photographed as described.

Received 4 November 1996; accepted 28 February 1997.

1. Cowan, W. M. *Development in the Nervous System* (Cambridge University Press, London, 1981).
2. Hatten, M. E. & Heintz, N. Mechanisms of neural patterning and specification in the developing cerebellum. *Annu. Rev. Neurosci.* **18,** 385–408 (1995).
3. Lane, P. W., Bronson, R. T. & Spencer, C. A. Rostral cerebellar malformation (*rcm*): A new recessive mutation on chromosome 3 of the mouse. *J. Hered.* **83,** 315–318 (1992).
4. Hedgecock, E. M., Culotti, J. G. & Hall, D. H. The *unc-5*, *unc-6*, and *unc-40* genes guide circumferential migrations of pioneer axons and mesodermal cells on the epidermis in *C. elegans*. *Neuron* **4,** 61–85 (1990).
5. Leung-Hagesteijn, C. *et al.* UNC-5, a transmembrane protein with immunoglobulin and thrombospondin type 1 domains, guides cell and pioneer axon migrations in *C. elegans*. *Cell* **71,** 289–299 (1992).
6. Hamelin, M., Zhou, Y., Su, M.-W., Scott, I. M. & Culotti, J. G. Expression of the UNC-5 guidance receptor in the touch neurons of *C. elegans* steers their axons dorsally. *Nature* **364,** 327–330 (1993).
7. Wadsworth, W. G., Bhatt, H. & Hedgecock, E. M. Neuroglia and pioneer neurons express UNC-6 to provide global and local netrin cues for guiding migrations in *C. elegans*. *Neuron* **16,** 36–46 (1996).
8. Leonardo, E. D. *et al.* Vertebrate homologues of *C. elegans* UNC-5 are candidate netrin receptors. *Nature* **386,** 833–838 (1997).
9. Akazawa, C. *et al.* A mammalian helix-loop-helix factor structurally related to the produce of *Drosophila* proneural gene *atonal* is a positive transcriptional regulator expressed in the developing nervous system. *J. Biol. Chem.* **270,** 8730–8738 (1995).
10. Ben-Arie, N. *et al.* Evolutionary conservation of sequence and expression of the bHLH protein Atonal suggests a conserved role in neurogenesis. *Hum. Mol. Gen.* **4,** 1207–1216 (1996).
11. Johnson, K. R., Cook, S. A. & Davisson, M. T. Chromosomal localization of the murine gene and two related sequences encoding high-mobility-group 1 and Y proteins. *Genomics* **12,** 503–509 (1992).
12. Willott, E. *et al.* The tight junction protein ZO-1 is homologous to the *Drosophila* discs-large tumor suppressor protein of septate junctions. *Proc. Natl Acad. Sci. USA* **90,** 7834–7838 (1993).
13. Serafini, T. *et al.* The netrins define a family of azon outgrowth-promoting proteins homologous to *C. elegans*. UNC-6. *Cell* **78,** 409–424 (1994).
14. Serafini, T. *et al.* Netrin-1 is required for commissural axon guidance in the developing vertebrate nervous system. *Cell* **87,** 1001–1014 (1996).
15. Livesey, F. J. & Hunt, S. P. Netrin and netrin receptor expression in the embryonic mammalian nervous system suggests roles in retinal, striatal, nigral and cerebellar development. *Mol. Cell. Neurosci.* (in the press).
16. Boyer, B. B. & Kozak, L. P. The mitochondrial uncoupling protein gene in brown fat: Correlation between DNase I hypersensitivity and expression in transgenic mice. *Mol. Cell. Biol.* **11,** 4147–4156 (1991).
17. Sternberg, N., Smoller, D. & Braden, T. Three new developments in P1 cloning. Increased cloning efficiency, improved clone recovery, and a new P1 mouse library. *Genet. Analyt. Tech. Appl.* **11,** 171–80 (1994).
18. Chomzynski, P. & Sacchi, N. Single-step method of RNA isolation by acid guanidinium thiocyanate–phenol–chloroform extraction. *Analyt. Biochem.* **162,** 156–159 (1987).
19. Sambrook, J., Fritsch, E. F. & Maniatis, T. *Molecular Cloning: A Laboratory Manual* (Cold Spring Harbor Laboratory Press, Cold Spring Harbor, New York, 1989).
20. Hui, C.-C. & Joyner, A. L. A mouse model of Greig cephalo-polysyndactyly syndrome: the *extra-toes*$_J$ mutation contains an intragenic detetion of the *Gli3* gene. *Nature Genet.* **3,** 241–245 (1993).
21. Kyte, J. & Doolittle, R. F. A simple method for displaying the hydropathic character of a protein. *J. Mol. Biol.* **157,** 105–132 (1982).
22. von Heijne, G. A new method for predicting signal sequence cleavage sites. *Nucleic Acids Res.* **14,** 4683–4690 (1986).
23. Klein, P., Kanehisa, M. & Delisi, C. The detection and classification of membrane-spanning proteins. *Biochim. Biophys. Acta.* **815,** 468–476 (1985).
24. Singer, S. F. The structure and insertion of integral proteins in membranes. *Annu. Rev. Cell Biol.* **6,** 247–296 (1990).

Acknowledgements. We thank K. Johnson for the mapping panel; H. Zoghbi for the *Math1* probe; R. Bronson and D. Goldowitz for discussion; E. Eicher, P. Nishina and M. Tessier-Lavigne for comments on the manuscript; D. McMinimy for DNA sequence analysis; and D. Frey for help with image analysis. This work was supported by grants from the NIH (to S.L.A., B.B.K., L.P.K. and L.A.R.) and a CORE grant from the National Cancer Institute.

Correspondence and requests for materials should be addressed to S.L.A. (e-mail: sla@aretha.jax.org).
Sequences have been deposited at GenBank, accession number U72634.